ELSEVIER

Materials Chemistry and Physics 78 (2002) 239–245

MATERIALS CHEMISTRY AND PHYSICS

www.elsevier.com/locate/matchemphys

Bandgap studies on anatase titanium dioxide nanoparticles☆

K. Madhusudan Reddy [a], Sunkara V. Manorama [a,*], A. Ramachandra Reddy [b]

[a] *Materials Science Group, Indian Institute of Chemical Technology, Hyderabad 500 007, Andhra Pradesh, India*
[b] *Physics Department, Regional Engineering College, Warangal, Andhra Pradesh, India*

Received 14 March 2002; received in revised form 9 May 2002; accepted 7 June 2002

Abstract

Titanium dioxide, predominantly in the anatase phase with an average grain size of 5–10 nm, has been synthesized by the hydrazine method. These nanocrystalline particles show a blue shift in the absorption edge of the diffuse reflectance ultraviolet spectrum of about 10 nm compared to that of commercially available titania. Synthesized samples were characterized by X-ray diffraction and transmission electron microscopy for their structural properties and UV-Vis absorption spectroscopy for the bandgap studies. The absorption spectra show a linear fit for the direct transition. The optical and electrical properties of the samples have been studied and the Arrhenius plots of electrical conductivity both for the as-prepared anatase TiO_2 and the one subsequently reduced in hydrogen atmosphere at 673 K show a distinct difference in the activation energy. The hydrogen-annealed sample shows a typical semiconducting behavior whereas the as-prepared sample indicates a phonon contribution to the conductivity around 300 K.

Keywords: Anatase titanium dioxide; Nanoparticles; Blue shift; Optical properties; Bandgap

1. Introduction

Titanium dioxide TiO_2 is a material with excellent merits in solar energy transferring and photocatalysis of poison compounds in environment [1]. Further, the strong oxidizing power of the photogenerated holes, the chemical inertness, and the non-toxicity of TiO_2 has also made it a superior photocatalyst [2–4]. The use of TiO_2 as a pigment in paints and the global oil crisis has inspired a variety of scientists and renewed interest in this material, and to the problem of using TiO_2 for splitting of water, based on the principles of photo-electrochemistry [5]. This material is known to exist in several forms, among them the most abundant are anatase, rutile and brookite [6]. The brookite phase is stable only at very low temperatures and hence not so useful practically. Rutile is the one that is obtained after high temperature calcination and its fundamental properties like the electrical, optical and thermal properties are well studied [7,8]. In contrast, the properties of the anatase form are not so well understood. The reason could be that the anatase, which is a comparatively low temperature stable phase, has gained significance only after nanostructured materials and their synthesis started playing a major role in materials science.

Nanostructuring of materials has opened up a new dimension and made size as a parameter to be considered for the phase diagrams in addition to the existing ones. The properties of nanosized semiconductor particles have been known to depend very sensitively on the particle size [9]. The physical properties of semiconductor nanocrystals are dominated by the spatial confinement of excitations (electronic and vibrational). Quantum confinement that manifests itself in widening of HOMO LUMO gap or the bandgap increase with decreasing crystallite size and its implications on the electronic structure and photophysics of the crystallites has generated considerable interest [10]. In order to synthesize nanoparticles and retain the size and morphology, it is mandatory to try and maintain sufficiently low temperatures during synthesis, processing and also in the course of application. In recent years anatase titania has also attracted a lot of interest because of its technological applications in paints, pigments and as a photocatalyst with promising efficiency but its application has been restricted because of the difficulty in synthesizing it in pure anatase form.

2. Experimental

TiO_2 nanoparticles were prepared by dropwise addition of 2 ml of 20% titanium tetrachloride (Loba Chemie) in hydrochloric acid to 500 ml of deionized water with vigorous stirring. Subsequently, 1.4 ml of hydrazine hydrate (100%)

☆ IICT Correspondence No.: 4569.

* Corresponding author. Tel.: +91-40-717-0921; fax: +91-40-7173-757/387.
E-mail address: manorama@iict.ap.nic.in (S.V. Manorama).

0254-0584/02/$ – see front matter
PII: S0254-0584(02)00343-7

(H_6N_2O, Ranbaxy) was added dropwise till the pH reached 8. The solution was stirred for further 4 h. The precipitate was filtered and dried at 80 °C overnight in air. The powder was dissolved in ethanol and subjected to ultra-sonication for 30 min to separate out the agglomerates formed. The powder was filtered and thereafter calcined at 400 °C for 2 h to get the crystalline titanium dioxide powder.

Bulk polycrystalline TiO_2 in the form of a commercial powder (Aldrich) (sample C) was taken as reference. The as-prepared TiO_2 (sample N) was characterized by X-ray diffraction (Seimens/D5000 diffractometer, X-ray radiation Cu Kα = 1.5406 Å) for the confirmation of structure and phase. The crystallite size was estimated by the line broadening using the Scherrer's equation. This polycrystalline TiO_2 is subjected to hydrogen annealing (sample H) for 15 min at 400 °C. Partial annealing in hydrogen atmosphere is carried out to create oxygen vacancies which we anticipate will increase the electrical conductivity of the sample. UV specular reflectance studies were performed on an UV absorption spectrophotometer (Hitachi 330) with a 3 nm slit width, response time 1 s with a speed of 120 nm min^{-1} to establish the type of band-to-band transition. Transmission electron micrographs (TEMs) were recorded on a JEOL JEM-100CX electron microscope. The electrical conductivity measurements were performed on an indigenously fabricated sample holder using a (Keithley 236/237) source measuring unit. The sample holder was equipped with a controlled sample heating and a temperature monitoring facility. Typical samples for the conductivity measurements were circular pellets with a diameter of 10 mm and thickness of 2 mm provided with conducting silver paste electrodes as electrical contacts. The results of the studies on the electrical and optical properties of the as-prepared sample are compared with those of sample C to establish our own reference values, and also highlight the advantages envisaged in obtaining the nanoparticles of TiO_2.

To demonstrate the quantum size effects in these ultrafine semiconductor particles immediately on synthesis, the particles were suspended in water and the UV absorption spectra recorded. The TiO_2 nanoparticles in suspension show the quantum size effect and the absorption edge shifts to lower wavelength when the particle size falls into nanometer range (<10 nm). It is observed that the absorption edge is noticeably blue shifted in comparison with that of the commercial sample (bandgap = 3.2 eV). From the shift in the absorption edge the particle size has been estimated using the equation as suggested by Wang and Herron [12] and found to be 7 nm.

3. Results and discussion

3.1. Shift in the X-ray diffraction peaks

The X-ray diffraction pattern of the as-prepared sample confirmed the pure anatase phase of the material. A closer look at Fig. 1, the position of the maximum intensity

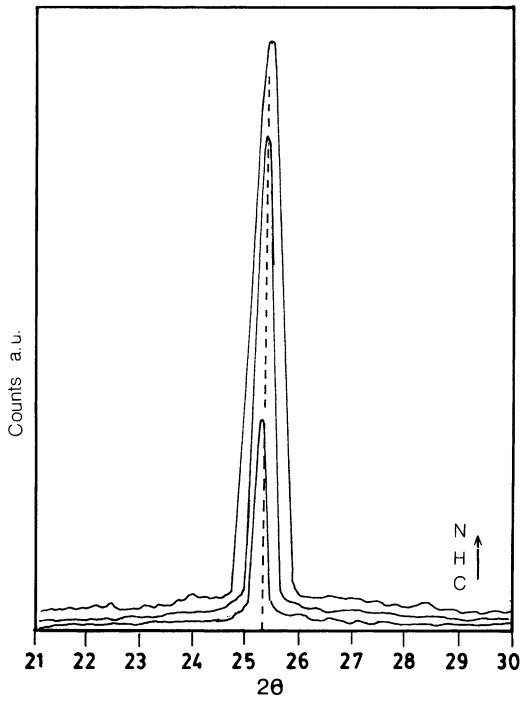

Fig. 1. XRD plot showing the peak shift for all the three samples.

(1 0 1) peak in the samples of TiO_2 whose diffraction features are qualitatively identical, reveals the peak shift from $\theta = 12.615°$ to 12.640° and 12.662° for samples C, H and N, respectively, corresponding to decreasing crystallite size. A clear shift of the peak to higher scattering angles with decreasing particle size is observed (Table 1).

Applying the Debye–Scherrer formula [11] and the full width at half maximum (FWHM) to the (1 0 1) reflection, typical values of crystallite sizes have been calculated to be in the range of 5–10 nm for the synthesized particles and as for the commercial sample it is about 39 nm. These are in agreement with the sizes estimated from scanning electron micrographs (SEMs) and TEMs. Fig. 2 shows a typical TEM of the nanoparticles of titanium dioxide with average particle size around 10–15 nm compared to the commercial one with particle size around 35–40 nm.

To substantiate our results an attempt is also being made to estimate the size dependent bandgap shift, ΔE_g from the following equation [12], using the average value of crystal-

Table 1
Tetragonal crystallite size, peak position and lattice parameters value for the C, H and N titania samples

Sample name	Crystallite size D_{XRD} (nm)	Peak position θ of (1 0 1) (°)	Lattice parameter (Å)	
			a	*c*
C	39	12.615	3.790	9.625
H	7.9	12.640	3.786	9.559
N	6.8	12.666	3.782	9.484

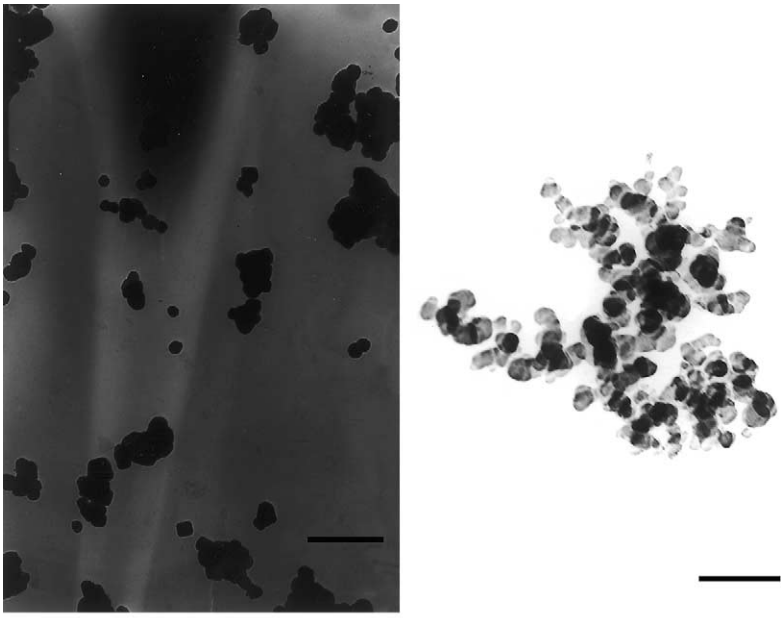

Fig. 2. TEMs (magnification 80K) of the TiO_2 nanoparticles (scale bar = 50 nm).

lite size as estimated from the Scherrer's formula:

$$\Delta E_g = \frac{h^2\pi^2}{2R^2}\left\{\frac{1}{m_e}+\frac{1}{m_h}\right\} - 1.786\frac{e^2}{\varepsilon R} - 0.248E^*_{RY} \quad (1)$$

where h is the reduced Planck's constant taken as 1.0545×10^{-34} J s, R the radius of the particle, E^*_{RY} the effective Rydberg energy calculated to be 4.3×10^{-39} J and ε is the dielectric constant of anatase $TiO_2 = 86$, m_e and m_h are the electron and hole masses, respectively. From this relation, ΔE_g for an average particle size of 5–10 nm is calculated to be around 0.1–0.2 eV. This provides an estimate for the bandgap E_g for the synthesized TiO_2 to be about 3.3–3.4 eV and for the commercial sample it is about 3.2 eV with a crystallite size of 39 nm.

Although there are several reports on the sizes of nanoparticles which show the quantum size effect, but what is the limit above which this phenomenon is observed is still not very clear. For example, there are reports like the one by Tora et al. [13] based on the photoacoustic intensity and phase spectra where the authors report that the energy gap of the anatase type TiO_2 powders with a particle size of 11 nm is 3.25 eV within the limits of experimental accuracy. They were able to show the quantum size effect with decreasing particle size. We have made an attempt to complement the blue shift observed from UV absorption studies with other results and draw some conclusions about the bandgap in these materials.

3.2. UV absorption study

Aqueous suspensions of the samples were used for the UV absorption studies. The blue shift that is observed in the absorption spectra with the decrease in particle size has been reported earlier [14]. The optical density plots that are obtained from the absorption spectra show a blue shift of about 10 nm for the samples N and H. Further, samples C, N and H were made into pellets with KBr and diffuse scattering UV recorded in the percentage absorption mode. Fig. 3 gives the diffused scattering UV-Vis spectra for the three samples. The bandgap of the sample C as calculated from the extrapolation of the absorption edge onto the energy axis is 3.2 eV and this is well reported.

Firstly, to establish the type of band-to-band transition in these synthesized particles, the absorption data were fitted to equations for both indirect and direct bandgap transitions. Fig. 4 shows the $\alpha^{1/2}$ versus E_{phot} plot for an indirect transition and Fig. 5 shows the $(\alpha E_{phot})^2$ versus E_{phot} for a direct transition, where α is the absorption coefficient and E_{phot} is the photon energy, $E_{phot} = (1239/\lambda)$ eV, where λ is the wavelength in nanometers. The value of E_{phot} extrapolated to $\alpha = 0$ gives an absorption energy, which corresponds to a bandgap E_g.

As seen in Fig. 4 for indirect transition the commercial sample shows a perfect fit and the extrapolation yields an E_g value of 3.2 eV which is in fact the bandgap of commercial titania. But for the samples N and H, the indirect fit plot yield bandgap values of 2.95 and 2.98 eV, respectively, which does not seem realistic. This is because for the samples with particle size 5–10 nm which is much less than the commercial particles (39 nm), there is always an increase in the bandgap energy. Hence their bandgap energy should be more than the 3.2 eV and not less as observed in the present case. The data is therefore fit to the direct bandgap relation and Fig. 5 shows the $(\alpha E_{phot})^2$ versus E_{phot} plots for these

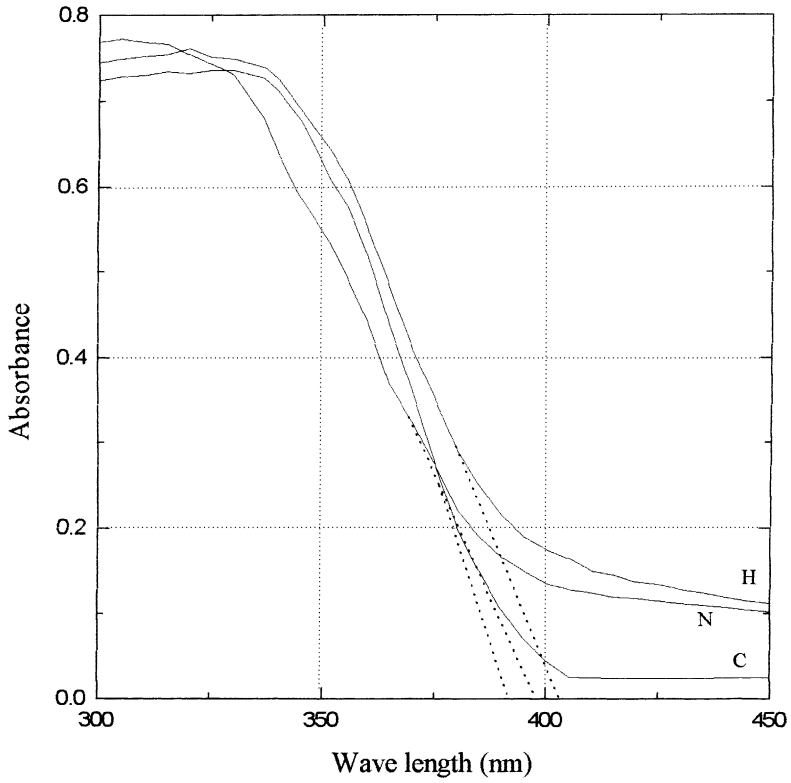

Fig. 3. Diffused UV absorption spectra of commercial (C), as-prepared (N) and hydrogen-annealed (H) samples.

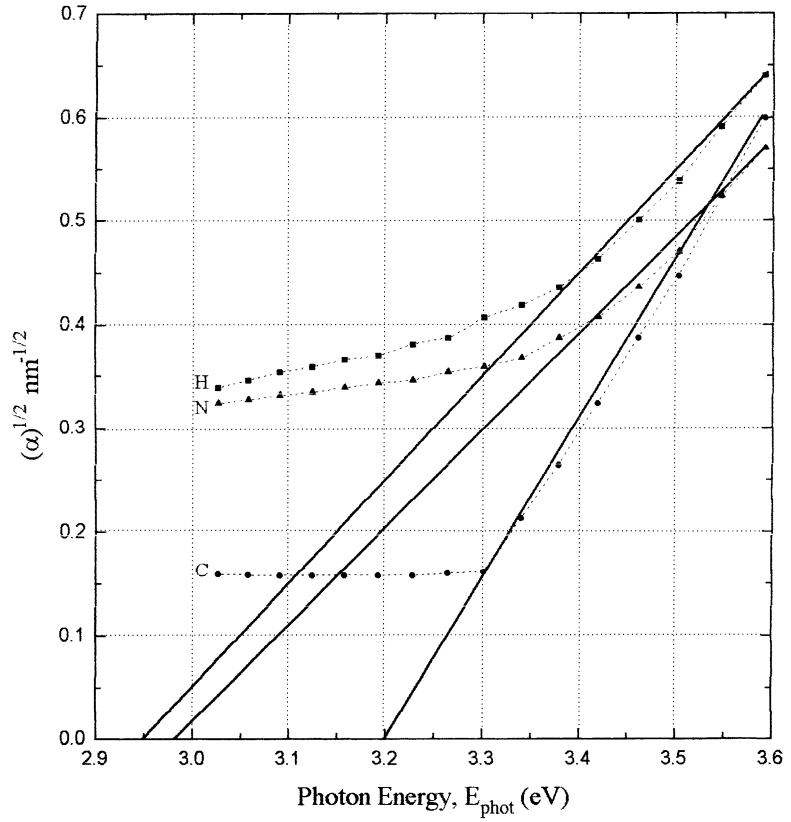

Fig. 4. Plot of $\alpha^{1/2}$ versus E_{phot} for indirect transition. Bandgaps E_g are obtained by extrapolation to $\alpha = 0$.

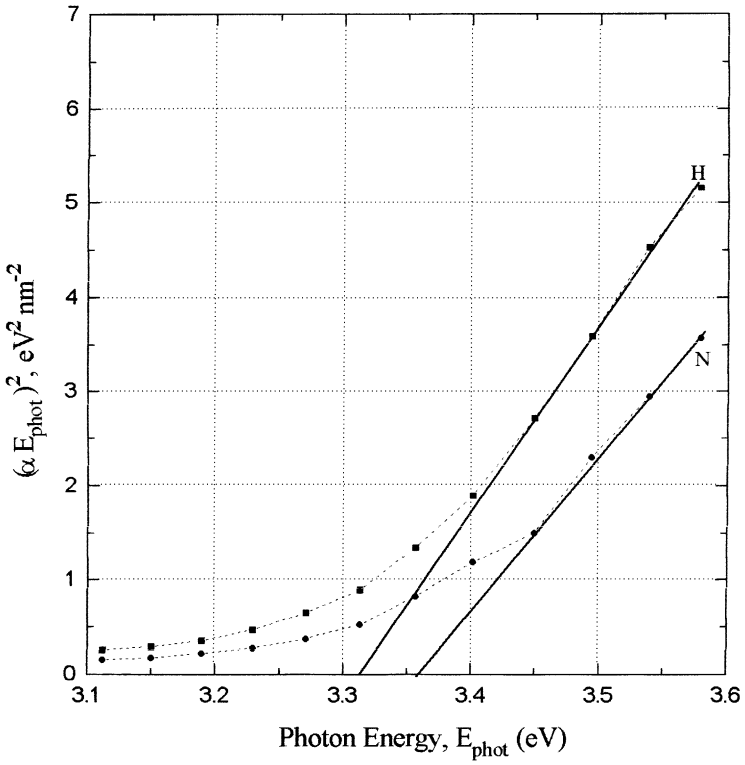

Fig. 5. Plot of $(\alpha E_{phot})^2$ versus E_{phot} for direct transition. Bandgaps E_g are obtained by extrapolation to $\alpha = 0$.

two samples. These data, which is a much better fit than the corresponding indirect bandgap fit, result in values of E_g estimated from the $\alpha = 0$ extrapolation as 3.36 eV for sample N and 3.32 eV for sample H.

As can be seen from the different E_g values, the bandgap shifts estimated for the synthesized nanoparticles from the plots for indirect transition are too large and therefore it could be inferred that the direct transition plots are more appropriate. This could be one reason to suggest that the direct, and not indirect transition, is more favorable in anatase TiO_2 nanoparticles. As opposed to this, there are a few reports where the nanoparticles have also been reported to follow an indirect transition as well [15].

For direct bandgap semiconductors, electronic transition from the valence band to the conduction band is electrical dipole allowed and the electronic absorption as well as emission is usually strong. For indirect bandgap semiconductors, the valence band to the conduction band electronic transition is electrical dipole forbidden and the transition is phonon assisted, i.e., both energy and momentum of the electron–hole pair are changed in the transition. Both their absorption and emission are weaker compared to those of direct bandgap semiconductors, since they involve a change in momentum. Hence a direct bandgap transition would result in a more efficient absorption of solar energy and therefore much better photovoltaic devices. Hence, any indication in this direction would direct towards a more favorable material for the applications envisaged.

Similar observations were made on Si nanocrystals where the quantum confinement causes a kinetic enhancement of the luminescence quantum yield, as well as an increase of the bandgap. Initially it was suggested that Si nanoparticles might be partially ‘direct-like’, as an explanation for the increased luminescence [16]. But subsequently, it was realized that it is not the increase in the radiative rate but the decrease in the non-radiative rate that is responsible for the high luminescence yield in Si nanocrystals and porous silicon with respect to bulk wafer Si. Similar size dependent changes have also been reported in indirect bandgap AgBr [17,18]. The results on silicon also suggest that we would also have to carry out photoluminescence studies to support our observations.

3.3. Electrical conductivity

To probe these materials further, the samples were subjected to electrical conductivity measurements from 300 to 673 K. Temperature dependence of the electrical conductivity σ is given by the Arrhenius equation, $\sigma = \sigma_0 \exp(-\Delta E/2kT)$ [19]. Fig. 6 shows the $\log \sigma$ versus $(1000/T)\,K^{-1}$ plots for samples N and H. TiO_2 when subjected to hydrogen annealing results in oxygen deficiency or vacancies which is responsible for increase in the conductivity. Cronemeyer [20] reported that the oxygen vacancies that exist in these kinds of materials could trap the excess electrons and thus the electrons associated with

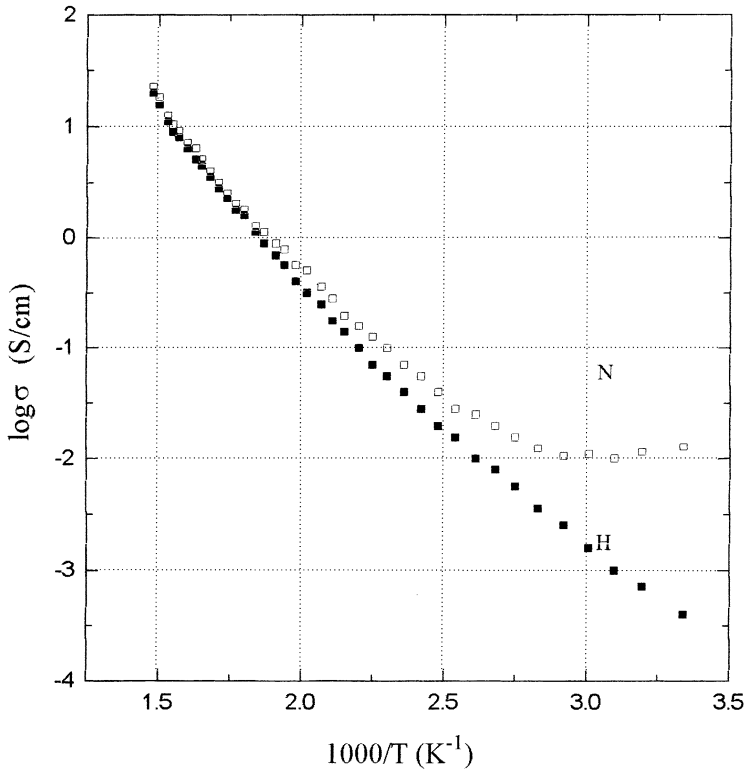

Fig. 6. $\log\sigma$ versus $(1/T)$ plot for electrical conductivity of nano-TiO_2 (N) and hydrogen-annealed TiO_2.

Ti^{4+} ions will have a much lower mobility than electrons in the conduction band. This would therefore indicate the existence of additional energy levels, intermediate between the normal valence and conduction bands, in lightly reduced anatase type TiO_2. In partly reduced TiO_2, oxygen vacancies are formed in the oxygen ion lattice which in turn ionize to form free electrons. Thus sample H would show a perfect semiconducting behavior and hence increase in conductivity with increasing temperature as expected. The activation energy calculated from the slope of the Arrhenius plot is about ~0.495 eV. For the similar plot sample N shows a peculiar behavior in the low temperature region. In the temperature range from 300 to 370 K, the conductivity decreases with temperature, which is indicative of a dominant phonon scattering phenomenon. Above 370 K the normal semiconducting behavior as in sample H is observed. Though there is not much data available on the electrical behavior of these nanoparticles, some similarities can be arrived at from the work on rutile TiO_2 [21,22]. Herein it has been observed that for lightly compensated samples, the temperature dependence of resistance leads to a higher conductivity as the temperature is lowered near 300 K quite similar to our observation.

4. Conclusion

In conclusion, we have the following results:

- Nanoparticles (5–10 nm) of pure anatase TiO_2 have been synthesized.
- The absorption coefficients α of the nanoparticle hydrogen-annealed and commercial sample has been obtained. These coefficients were used to determine the type of band-to-band transition using plots of $(\alpha E_{phot})^2$ versus E_{phot} and $\alpha^{1/2}$ versus E_{phot} for direct and indirect transition, respectively. The commercial sample as expected shows an indirect transition, whereas nano-TiO_2 shows a direct transition.
- The electronic conductivity measurements for the hydrogen-annealed sample shows a normal semiconductor behavior that can be attributed to the formation of vacancies, whereas the nano-TiO_2 gives an indication of dominant phonon scattering phenomena at low temperatures and normal semiconducting behavior at high temperatures.
- Experiments are underway to explain the observation of the partially direct bandgap in terms of luminescence studies and also carrying out suitable photovoltaic and photocatalytic reactions that would demonstrate an improved efficiency in terms of the yield and selectivity.

References

[1] M.R. Hoffmann, S.T. Martin, W. Choi, D.W. Bahnemann, Chem. Rev. 95 (1995) 69.

[2] D.G. Fu, Y. Zhang, X. Wang, J.Z. Liu, Z.H. Lu, Chem. Lett. (2001) 328–329.
[3] F.A. Grant, Rev. Mod. Phys. 31 (1959) 646.
[4] H.P.R. Frederiske, J. Appl. Phys. 32 (Suppl.) (1961) 2211.
[5] G. Schmid, M. Baumle, M. Greekens, I. Heim, C. Osemann, T. Sawatowski, Chem. Soc. Rev. 28 (1999) 179–185.
[6] C.B. Murray, D.J. Norris, M.G. Bawendi, J. Am. Chem. Soc. 115 (1993) 8706.
[7] Q. Zhang, L. Gao, J. Guo, Appl. Catal. B 26 (2000) 207–215.
[8] M.A. Fox, M.T. Dulay, Chem. Rev. 93 (1993) 341–357.
[9] A.L. Linsebigler, G. Lu Jr., J.T. Yatus, J. Phys. Chem. 99 (1995) 7626–7631.
[10] A. Fujishima, K. Honda, Nature 238 (1972) 37–38.
[11] B.D. Cullity, Elements of X-ray Diffraction, Addison-Wesley, Reading, MA, 1978.
[12] Y. Wang, N. Herron, J. Phys. Chem. 95 (1991) 525–532.
[13] T. Tora, K. Hiroshi, S. Qing, K. Akihik, O. Masahiro, Jpn. J. Appl. Phy. Part 1 39 (5B) (2000) 3160–3164.
[14] K. Madhusudan Reddy, C.V. Gopal Reddy, S.V. Manorama, J. Sol. State Chem. 158 (2001) 180–186.
[15] C.A. Hogarth, Z.T. Al-Dhhan, Phys. Status Sol. B 137 (1986) K157.
[16] L. Brus, J. Phys. Chem. Solids 59 (1998) 459–465.
[17] A.P. Marchetti, K.P. Johansson, G.P. McLendon, Phys. Rev. B 47 (1993) 4268.
[18] H. Kanzaki, Y. Tadakuma, Sol. State Commun. 80 (1991) 33–36.
[19] R. Smith, Semiconductors, Cambridge University Press, London, 1980.
[20] D.C. Cronemeyer, Phys. Rev. 113 (1959) 1222.
[21] R.G. Breckneridge, W.R. Hosler, Phys. Rev. 91 (1953) 793–802.
[22] J.H. Beccer, W.R. Hosler, Phys. Rev. 137 (6A) (1965) 1872–1877.